Statistical investigation of the saturation effect in the ionospheric foF2 versus sunspot, solar radio noise, and solar EUV radiation

J. Y. Liu
Institute of Space Science and Center for Space and Remote Sensing Research, National Central University, Chung-Li, Taiwan

Y. I. Chen and J. S. Lin
Institute of Statistics, National Central University, Chung-Li, Taiwan

Received 17 July 2001; revised 28 April 2002; accepted 12 June 2002; published 7 February 2003.

[1] This study explores the saturation effects in the ionospheric foF2 due to sunspot number *R*, solar radio noise (10.7 cm) flux F10.7, and solar EUV fluxes. To locate the *R*, F10.7, or EUV value at which the foF2 values are saturated, a two-segmented regression model is built based on the data of the strictly rise period of the 21st solar cycle recorded by eight ionosonde stations scattering roughly between 40°N and 40°S geomagnetic latitude. Results show that clear saturation features appear around the equatorial anomaly crest regions. The regression model is then fitted into the foF2 data observed at Chung-Li station (13.8°N, geomagnetic) to investigate the hourly variation of the saturation effect. The saturated foF2 slope and the value of the *R* or EUV at which the foF2 values are saturated in the fitted models are closely related to the overall mean and standard deviation of foF2. The hourly results demonstrate that the daily ionospheric equatorial fountain and prereversal enhancement are important for the saturation features. *INDEX TERMS:* 2479 Ionosphere: Solar radiation and cosmic ray effects; 6929 Radio Science: Ionospheric physics (2409); 2437 Ionosphere: Ionospheric dynamics; 2479 Ionosphere: Solar radiation and cosmic ray effects; *KEYWORDS:* saturation effect, ionospheric foF2, sunspot number, solar radio noise, solar EUV radiation

Citation: Liu, J. Y., Y. I. Chen, and J. S. Lin, Statistical investigation of the saturation effect in the ionospheric foF2 versus sunspot, solar radio noise, and solar EUV radiation, *J. Geophys. Res.*, *108*(A2), 1067, doi:10.1029/2001JA007543, 2003.

1. Introduction

[2] Ionospheric electron densities are produced mainly by solar EUV and X-ray radiations, which are known to vary with long periods (e.g., solar cycle) and also with short periods (e.g., solar flares). The long, continuous but manually observed data of sunspot numbers are often used to study the ionosphere response to the solar activity. *Gopala Rao and Samibasiva Rao* [1969] and *Davies* [1990] find for the same sunspot number that the penetration frequency of the ionosphere foF2 might show different values during the rise and fall periods of the solar cycle. Scientists observe that foF2 shows a good linear relationship for low values of the sunspot numbers, but foF2 seems to show a saturation effect at high sunspot numbers (for example see, [*Lakshmi et al.*, 1988]). *Jones and Obitts* [1970] fit a parabolic law to the solar-cycle variation of foF2 and find more saturation at the higher solar epochs. However, it remains the problem of determining the sunspot number *R* where the foF2 values are saturated. By examining the relationship between the monthly median noon foF2 value and smoothed (12-month running mean) sunspot number R_{12} in equinoxes and summer months, respectively, in the rise period of the 21st solar cycle, *Kane* [1992] further points out that this "hysteresis" effect is small at low and high latitudes but substantial at middle latitudes. Although the separated analyses of foF2 recorded in equinoxes and summer months could remove the seasonal effects, *Kane* [1992] suffers with limited grouped data and still does not provide any information about the smoothed sunspot number at which foF2 is saturated. Meanwhile, *Balan et al.* [1993, 1994a, 1994b, 1996] modelingly analyze the relationship between ionospheric ionization, solar radio noise (10.7 cm) flux F10.7, and solar EUV during intense solar cycles. They find a nonlinear relationship between the solar EUV and F10.7 and consider the saturation of ionization to be caused by the saturated production of ionization due to the nonlinear increase of the solar EUV fluxes. To quantitatively determine the saturated effect, *Chen et al.* [2000] study the noontime foF2 simulated by the International Reference Ionosphere IRI90 [*Bilitza*, 1990] and observed at Chung-Li station (13.8°N, geomagnetic). They show that the solar cycle variation of either simulated or observed foF2 can be well represented by a pair of lines, and the change point in the two-segmented linear regression model can be estimated which is the value of R_{12} where foF2 is saturated.

[3] In this paper, instead of modeled data, we analyze the saturation effects in observations of the foF2 versus the sunspot number *R*, the foF2 versus the solar radio flux

0148-0227/03/2001JA007543$09.00

F10.7, and the foF2 versus the solar EUV flux. Since the solar EUV flux is only available during the full Atmospheric Explorer-E satellite (AE-E) mission (1 July 1977 through 30 December 1980) [*Hedin*, 1984; *Tobiska and Barth*, 1990], we isolate the F10.7 solar radio flux and sunspot number R stored at the world data center (CD ROM database, NGDC-05) as well as the foF2 recorded by several ionosondes during the same period. To avoid the seasonal variation, we employ a 12-month running mean, which has been used to derive the well-known R_{12} on measurements of the monthly median foF2, monthly mean F10.7, and monthly mean EUV values to obtain their associated 12-month running mean $foF2_{12}$, $F10.7_{12}$, and EUV_{12}, respectively. For a quantitative examination the two-segmented linear regression model [*Chen et al.*, 2000] is adopted herein to describe the relationship between the $foF2_{12}$ and the three solar parameters. First, to locate where the most profound saturation effects occur, we examined the noontime $foF2_{12}$ observed from eight ionosonde stations evenly lying between 40°N and 40°S geomagnetic latitudes. Later, the diurnal variations of the most profound effects are further investigated. Finally, possible mechanisms related the saturation effects are proposed and discussed.

2. Method

[4] A two-segmented linear regression model with unknown change-point c is a regression model

$$y_t = f(x_t, c, \beta) + e_t, \qquad t = 1, 2, \ldots, n,$$

where the response function $f(x_t, c, \beta)$ has the following form:

$$\begin{aligned} f(x, c, \beta) &= f_1(x, \beta_1), \qquad x \le c, \\ &= f_2(x, \beta_2), \qquad x > c, \end{aligned}$$

the $f_i(x, \beta_i)$s being linear functions of x involving a vector of unknown parameters, β_is. The error terms e_t are assumed to be independent Gaussian variables with mean zero and finite variance σ^2.

[5] In our application the response variable, y, is the $foF2_{12}$, the smoothed monthly median noon foF2 value. We examine its relationship with x, the smoothed R_{12}, $F10.7_{12}$, or EUV_{12}.

[6] For describing the saturation effect in $foF2_{12}$ the reparameterized model is considered

$$f(x; \boldsymbol{\theta}) = \theta_1 + \theta_2(\theta_3 - x)\, I(\theta_3 - x),$$

where $I(z) = 1$, if $z \ge 0$, and $I(z) = 0$, otherwise. Note that θ_3 is the change point, θ_1 represents the expected y value when x is greater than θ_3, and $-\theta_2$ is the slope or changing rate of the first segmented linear regression model. The least-squares estimates of $\theta = (\theta_1, \theta_2, \theta_3)$, denoted by $\hat{\boldsymbol{\theta}} = (\hat{\theta}_1, \hat{\theta}_2, \hat{\theta}_3)$, minimizes

$$Q(\boldsymbol{\theta}) = \sum_{t=1}^{n} [y_t - f(x_t; \boldsymbol{\theta})]^2$$

can be found using the modified Gauss-Newton algorithm as described by *Gallant and Fuller* [1973]. The corresponding residual sum of squares is then obtained as $RSS(SL) = Q(\hat{\boldsymbol{\theta}})$ and the fitted two-segmented linear regression model is

$$\hat{y} = \hat{\theta}_1 + \hat{\theta}_2\hat{\theta}_3 - \hat{\theta}_2 x, \qquad x \le \hat{\theta}_3,$$

and

$$\hat{y} = \hat{\theta}_1, \qquad x > \hat{\theta}_3.$$

[7] To test the goodness-of-fit for the two-segmented linear regression model, a simple linear regression model is also fitted into the data under study and the related residual sum of squares is obtained as RSS(L). Note that under the Gaussian distribution, the distribution of the statistic

$$F = \{(n-3)\mathrm{RSS(L)}\}/\{(n-2)\mathrm{RSS(SL)}\}$$

is the F distribution with degrees of freedom $n - 2$ and $n - 3$, denoted by $F(n - 2, n - 3)$. Therefore if the F value is greater than the upper 1st percentile of $F(n - 2, n - 3)$, then at the significance level 0.01 the two-segmented linear regression model is claimed to be better than the simple linear regression model for fitting the data under study. In other words, a saturation effect in $foF2_{12}$ is declared when R_{12}, $F10.7_{12}$, or EUV_{12} is equal to or larger than $\hat{\theta}_3$.

3. Data Analysis and Results

[8] A survey of the CD-ROM database published by the World Data Center shows that the most complete data set and the most profound saturated effect in foF2 are recorded in period of the 21st solar cycle. Note that the strictly rise period of the cycle is from January 1977–June 1979 while the full AE-E mission (15 wavelength groups lie between 168 and 1216 Å) starts from 1 July 1977. Therefore there is an EUV data gap between January and June 1997. Fortunately, we found the observed EUV of 530.9 Å starts as early as January 1976. To validate if the EUV (530.9 Å) could well represent the overall EUV variations, we further compare it with the integrated solar EUV flux (168–1026 Å) computed from a solar EUV flux model SERF2 by the Solar Electromagnetic Radiation Flux study [*Tobiska and Barth*, 1990]. A linear relationship between the two indicates that the observed EUV (530.9Å) is suitable and can be adopted in this study. Figure 1 displays the R_{12}, $F10.7_{12}$, and EUV_{12} recorded during the strictly rise period of the cycle (January 1977–June 1979). We find that the tendencies in the R_{12} and $F10.7_{12}$ variations are linearly correlated. Therefore for simplicity only the relationships of $foF2_{12}$-R_{12}, and $foF2_{12}$-EUV_{12} are investigated in further detail.

[9] The foF2 values analyzed in this paper were recorded at eight ionosonde stations (geomagnetic latitudes), including Karaganda (40.3°N), Maui (21.0°N), Chung-Li (13.8°N), Manila (3.5°N), Huancayo (0.7°S), Tahiti (15.3°S), Townsville (28.6°S), and Canberra (43.8°S). Therefore for each parameter under study, there are $n = 30$ pairs of observations

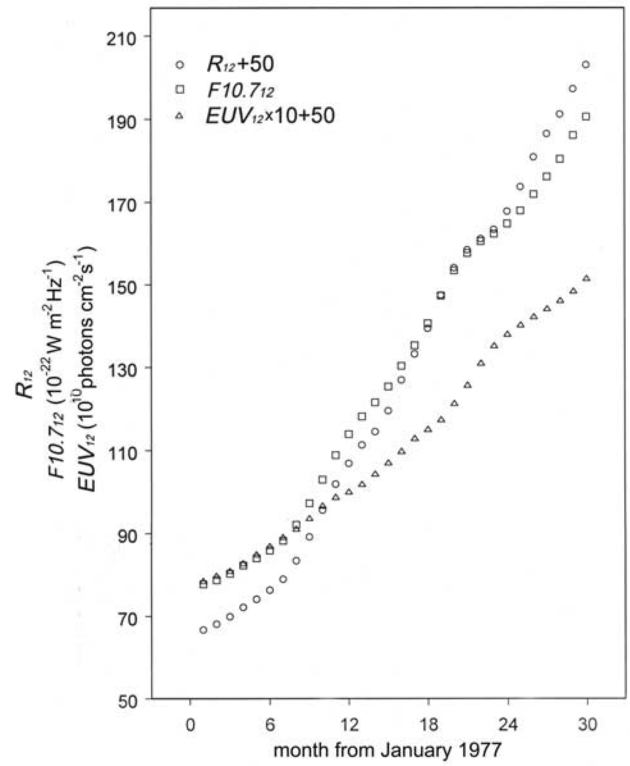

Figure 1. The R_{12}, F10.7$_{12}$, and EUV$_{12}$ recorded during the strictly rise period of the 21st cycle, January 1977 to June 1979.

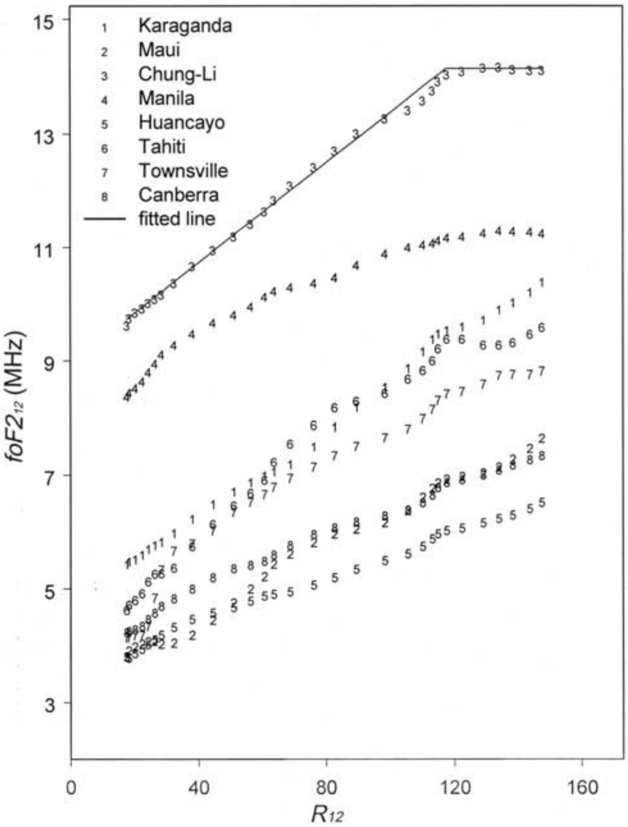

Figure 2. Plots foF2$_{12}$ versus R_{12} during January 1977–June 1979.

in each station. The plots of noontime foF2$_{12}$ versus R_{12} and foF2$_{12}$ versus EUV$_{12}$ for the eight stations are given in Figures 2 and 3 respectively.

[10] The goodness-of-fit F values for the eight stations of the two investigations reported in Tables 1 and 2, respectively, show that the significant saturation effect in the smoothed foF2$_{12}$ values appear in Tahiti and Chung-Li. Figure 4 displays the mean of the noontime foF2$_{12}$ as well as the F values of the R_{12} and EUV$_{12}$ of the eight stations in the geomagnetic latitude coordinate during January 1977–June 1979. It can be seen that the three quantities simultaneously reach two maxima at Tahiti and Chung-Li, where are around the southern and northern equatorial anomaly regions (for example see *Ratcliffe* [1974]), respectively. The fitted two-segmented linear regression models for both the saturated stations presented in Tables 3 and 4 reveal that the saturated foF2$_{12}$ values $\hat{\theta}_1$ with R_{12} (EUV$_{12}$) are 14.16 (14.12) MHz at Chung-Li and 9.42 (9.61) MHz at Tahiti which occurred at the change points $\hat{\theta}_3$; namely, the R_{12} (EUV$_{12}$) values 118.6 (7.84) and 115.3 (8.58 10^{10} photons cm^{-2} s^{-1}), respectively. Moreover, the two slopes, $-\hat{\theta}_2$, of the R_{12} (EUV$_{12}$) before the saturation are similar, which are 0.043 (0.92) and 0.047 MHz (0.85 MHz/(10^{10} photons cm^{-2} s^{-1})) for Chung-Li and Tahiti, respectively. It can be seen from the F values in Tables 1 and 2 that the most profound saturation effect in the relationship between R_{12} and foF2$_{12}$ as well as EUV$_{12}$ and foF2$_{12}$ is observed at Chung-Li. Plots of foF2$_{12}$ versus R_{12} and foF2$_{12}$ versus EUV$_{12}$ together with the associated fitted two-segmented linear regression models at Chung-Li are then demonstrated by segmented solid lines in Figures 2 and 3, respectively.

[11] To further understand the diurnal variation of the saturation effects observed at Chung-Li, we compute and present in Table 5 the mean value and standard deviation of foF2$_{12}$, the F values as well as the saturated foF2$_{12}$, slope, and changing point in the fitted two-segmented linear regression model for various local time (LT) during January 1977–June 1979. Note that hereafter the foF2$_{12}$ denotes the 12-month running of the monthly median on top of each local hour. It is found that at the significance level 0.01, clear saturation effects in foF2$_{12}$ versus R_{12} and foF2$_{12}$ versus EUV$_{12}$, appear between 1000 and 2100 LT. Notice that the slopes, $-\hat{\theta}_2$, from 2200 to 0900 LT, when the F values are not significant, are estimated by the first segmented of the model. Figure 5 displays the mean values of the foF2$_{12}$ and their associated standard deviations (SDs), which are significantly different at 1300 and 2100 LT. It is surprising to find that at ~1400–1500 LT, the mean is the maximum while the standard deviation yields a minimum. Figures 6 and 7 present the relationship between the mean and the saturation quantities in foF2$_{12}$ versus R_{12} and foF2$_{12}$ versus EUV$_{12}$, respectively. It is interesting to note that the saturated foF2$_{12}$ is proportional to the mean, while the change point R_{12} (or EUV$_{12}$) is inversely proportional to the two quantities. The dissimilarity is that the F values for foF2$_{12}$ versus R_{12} and foF2$_{12}$ versus EUV$_{12}$ yield two maxima, at 1200 and 1800 LT and at 1500 and 2000 LT, respectively (also see Table 5). Figure 8 illustrates the slopes in foF2$_{12}$ versus R_{12} and foF2$_{12}$ versus

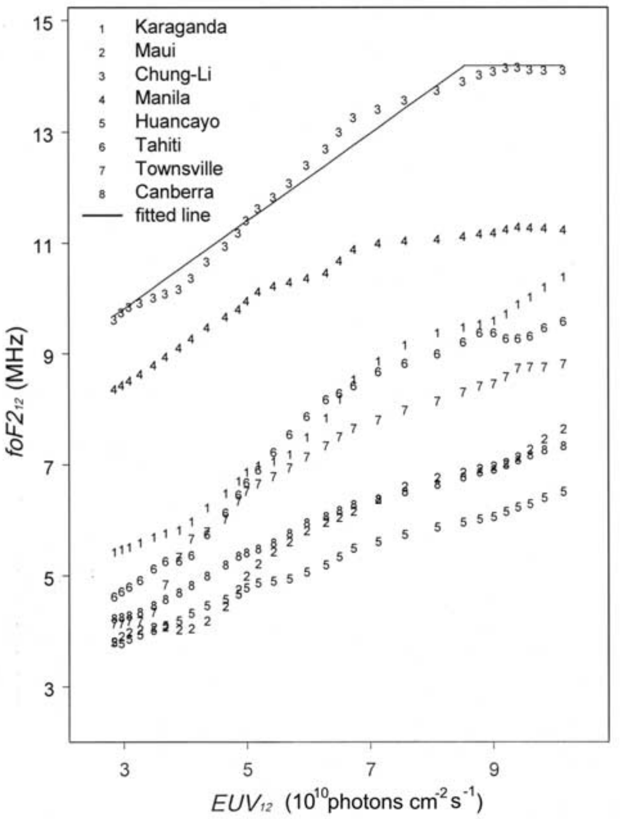

Figure 3. Plots foF2$_{12}$ versus EUV$_{12}$ during January 1977–June 1979.

EUV$_{12}$ and the standard deviation of the foF2$_{12}$ to be highly correlated.

4. Discussion and Conclusion

[12] *Balan et al.* [1993, 1994a, 1994b, 1996] modelingly studied variations of the ionosphere and related solar fluxes during intense solar cycles and found that ionospheric electron density responded linearly to the solar EUV fluxes but nonlinearly to the solar F10.7. They interpreted that the saturated effect in ionospheric electron density was due to a nonlinear relationship between solar EUV and F10.7 fluxes. Figure 1 also reveals the nonlinear relationship between solar EUV$_{12}$ and F10.7$_{12}$ (or R_{12}). However, the significant F values of foF2$_{12}$ versus EUV$_{12}$ suggest that the nonlinear relationship proposed by *Balan et al.* [1993, 1994a, 1994b, 1996] might not be able to fully explain the saturation effect.

Table 1. Goodness-of-Fit F Value for Two-Segmented Linear Regression Models With R_{12}

Station	Geomagnetic Latitude	RSS(L)	RSS(SL)	F
Karaganda	40.3°N	0.71	0.59	1.167
Maui	21.0°N	0.70	0.64	1.064
Chung-Li	13.8°N	2.81	0.30	9.031[a]
Manila	3.5°N	2.22	0.69	3.089[a]
Huancayo	0.7°S	0.18	0.16	1.083
Tahiti	15.3°S	4.01	0.65	5.936[a]
Townsville	28.6°S	4.41	2.63	1.615
Canberra	43.8°S	0.42	0.28	1.445

[a]Significance level 0.01.

Table 2. Goodness-of-Fit F Value for Two-Segmented Linear Regression ModelsWith EUV$_{12}$

Station	Geomagnetic Latitude	RSS(L)	RSS(SL)	F
Karaganda	40.3°N	1.16	1.1	1.012
Maui	21.0°N	1.43	1.35	1.028
Chung-Li	13.8°N	3.96	0.63	6.110[a]
Manila	3.5°N	2.73	2.45	1.073
Huancayo	0.7°S	0.22	0.22	0.987
Tahiti	15.3°S	5.51	2.33	2.283[a]
Townsville	28.6°S	5.07	4.01	1.22
Canberra	43.8°S	0.64	0.46	1.354

[a]Significance level 0.01.

[13] The agreement between the foF2$_{12}$ versus R_{12} and foF2$_{12}$ versus EUV$_{12}$ plots and their associated models at Chung-Li shown in Figures 2 and 3, respectively, demonstrates that the two-segmented linear model well describes the foF2 saturation feature. Results in Tables 1 and 2 as well as in Figure 4 show that the most clear saturation effect occurs around the equatorial anomaly region where the ionospheric density (or plasma frequency foF2) generally yields a maximum value (for example, *Ratcliffe* [1974]). Note that the mean of the noontime foF2$_{12}$ during January 1977–June 1979 at Chung-Li and Tahiti yield local maximum values in the Northern and Southern Hemispheres, respectively (see Figure 4). It is also interesting to find that the mean of the noontime foF2$_{12}$ at Chung-Li is much greater than that at Tahiti while the F values for both R_{12}

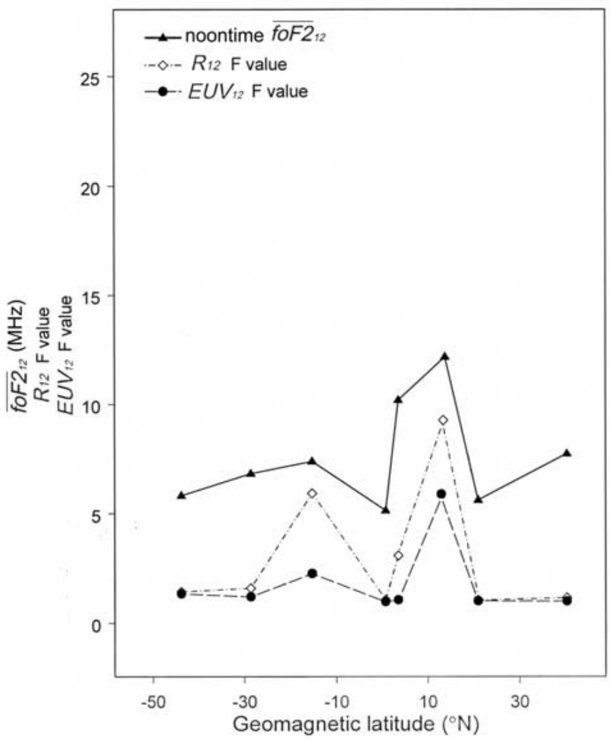

Figure 4. The mean of the noontime foF2$_{12}$ and F values of R_{12} and EUV$_{12}$ in various geomagnetic latitudes during January 1977–June 1979.

Table 3. Fitted Two-Segmented Linear Regression Models With R_{12}

Station	Geomagnetic Latitude	$\hat{\theta}_1$	$\hat{\theta}_2$	$\hat{\theta}_3$
Chung-Li	13.8°N	14.16	−0.043	118.6
		y = 8.97 + 0.043 x		if x ≤ 118.6
		= 14.16		x > 118.6
Tahiti	15.3°N	9.42	−0.047	115.3
		y = 4 + 0.047 x		if x ≤ 115.3
		= 9.42		x > 115.3

and EUV_{12} at Tahiti is not so predominant. Thus it is a reasonable to conjecture that in particular at which the foF2 has a great value, the ionosphere can be easily filled up and become saturated.

[14] Figure 5 reveals at 1300–1500 LT that the $foF2_{12}$ mean reaches the maximum while the associated standard deviation yields a minimum. This suggests that the ionosphere has a limited electron density capacity and during the postnoon period that owing to the dense ambient electron density, it becomes less fluctuated and approaches saturated. Meanwhile, also owing to the dense electron density, the *F* values in the $foF2_{12}$ versus R_{12} (Figure 6) and $foF2_{12}$ versus EUV_{12} (Figure 7) reach their maxima at 1200 LT and 1500 LT, respectively.

[15] To precisely and quantitatively determine the changing and saturated points as well as the goodness of fit of the saturation effects (*F* value), the 12-month running mean has been applied on all the observations used in this study. Therefore the current study does not examine the seasonal effects. However, by contrast, *Kane* [1992] studied the relationship between EUV, F10.7, and R_{12} versus monthly median of noontime foF2 in equinoxes and summer of 1977–1980. Although the saturated quantities were not reported in detail, his results show that during the dense electron density seasons of the equinoxes months, more banded curves (or the saturation features) appear. On the basis of the latitudinal and diurnal results in Figures 46–7 and the seasonal study of *Kane* [1992], it can be summarized that the ionosphere with a denser ambient electron density might have a better chance to become saturated.

[16] The greatest ionospheric electron density usually occurs around the equatorial anomaly regions [*Davies*, 1990]. The latitudinal results in Figure 4 reveal that the most profound saturation effects occur also in the equatorial anomaly region. It has been known that the electron density in the region could also be variable in terms of several factors like solar activity, as well as longitude, season, and neutral

Table 4. Fitted Two-Segmented Linear Regression Models With EUV_{12}

Station	Geomagnetic Latitude	$\hat{\theta}_1$	$\hat{\theta}_2$	$\hat{\theta}_3$
Chung-Li	13.8°N	14.12	−0.92	7.84
		y = 7.44 + 0.92 x		if x ≤ 7.84
		= 14.12		x > 7.84
Tahiti	15.3°N	9.61	−0.85	8.58
		y = 2.32 + 0.85 x		if x ≤ 8.58
		= 9.61		x > 8.58

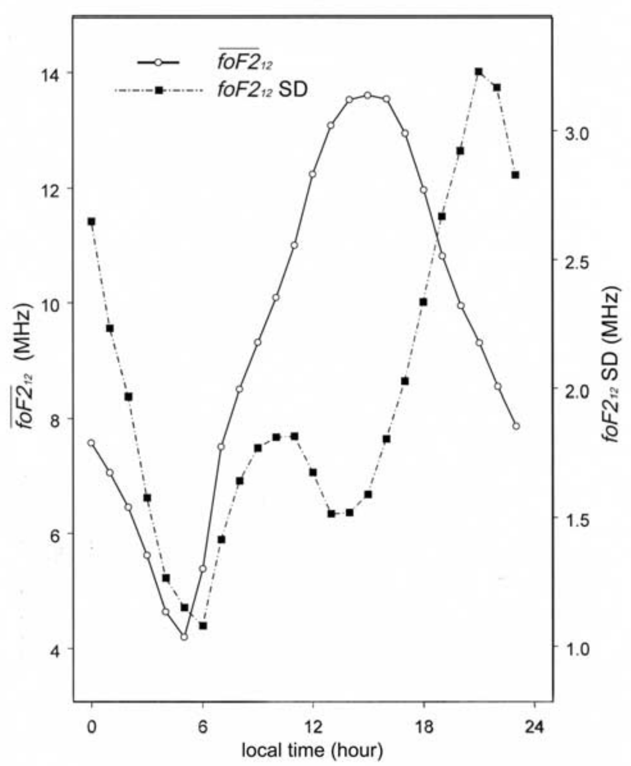

Figure 5. The diurnal variations in the mean $foF2_{12}$ and associated standard deviation, SD, at Chung-Li during January 1977–June 1979.

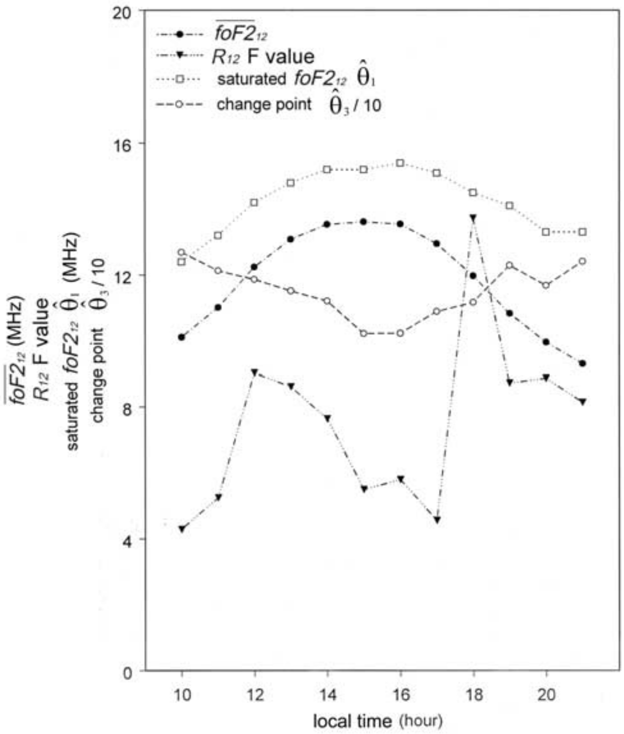

Figure 6. The mean $foF2_{12}$ and the *F* value, saturated point $\hat{\theta}_1$, and changing point $\hat{\theta}_3$ for $foF2_{12}$ versus R_{12} at various Taiwan local times during January 1977–June 1979.

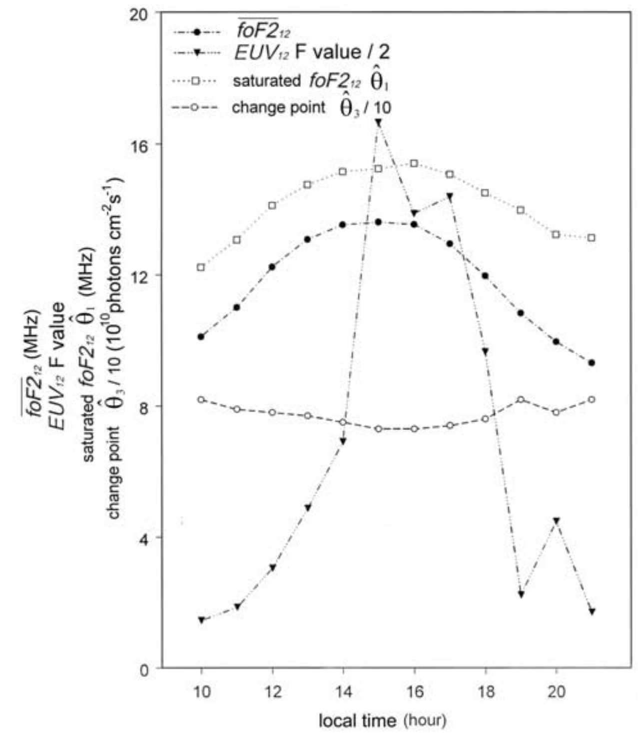

Figure 7. The mean $foF2_{12}$ and the F value, saturated point $\hat{\theta}_1$, and changing point for $\hat{\theta}_3$ $foF2_{12}$ versus EUV_{12} at various Taiwan local times during January 1977–June 1979.

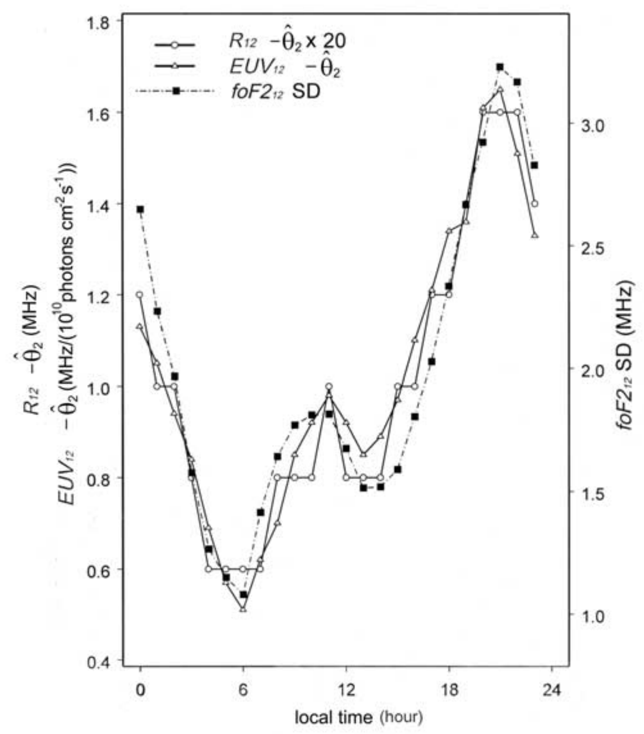

Figure 8. The diurnal variations in the $foF2_{12}$ standard deviation, SD, as well as the slopes $-\hat{\theta}_2$ for $foF2_{12}$ versus R_{12} and $foF2_{12}$ versus EUV_{12} at Chung-Li during January 1977–June 1979.

Table 5. Summary Statistics, F Values, and the Fitted Two-Segmented Linear Regression Models with R_{12} and EUV_{12} at Chung-Li

$foF2_{12}$			R_{12}				EUV_{12}			
LT, hhmm	Mean, MHz	SD, MHz	F value	$\hat{\theta}_1$, MHz	$-\hat{\theta}_2$, MHz/[a]	$\hat{\theta}_3$[a]	F value	$\hat{\theta}_1$, MHz	$-\hat{\theta}_2$, MHz/[b]	$\hat{\theta}_3$[b]
0000	7.57	2.65	0.98		0.061		0.99		1.13	
0100	7.06	2.23	1.23		0.052		1.14		1.05	
0200	6.46	1.97	1.91		0.047		1.36		0.94	
0300	5.62	1.58	1.35		0.038		1.6		0.84	
0400	4.64	1.27	1.31		0.031		1.85		0.69	
0500	4.2	1.15	1.26		0.028		1.44		0.57	
0600	5.39	1.08	1.19		0.025		1.26		0.51	
0700	7.5	1.41	1.21		0.033		1.12		0.62	
0800	8.5	1.64	0.96		0.038		1		0.7	
0900	9.31	1.77	1.72		0.042		1.83		0.85	
1000	10.1	1.81	4.29[c]	12.4	0.044	126.9	2.90[c]	12.23	0.92	8.2
1100	11	1.81	5.25[c]	13.2	0.046	121.3	3.72[c]	13.07	0.98	7.9
1200	12.24	1.68	9.03[c]	14.2	0.043	118.6	6.11[c]	14.12	0.92	7.8
1300	13.08	1.51	8.62[c]	14.8	0.04	115.1	9.74[c]	14.76	0.85	7.7
1400	13.53	1.52	7.64[c]	15.2	0.041	112	13.82[c]	15.16	0.89	7.5
1500	13.61	1.59	5.50[c]	15.2	0.047	102.1	33.32[c]	15.25	0.97	7.3
1600	13.54	1.8	5.80[c]	15.4	0.054	102.2	27.75[c]	15.41	1.1	7.3
1700	12.95	2.03	4.56[c]	15.1	0.056	108.8	28.78[c]	15.08	1.21	7.4
1800	11.97	2.33	13.72[c]	14.5	0.063	111.6	19.28[c]	14.51	1.34	7.6
1900	10.82	2.67	8.73[c]	14.1	0.067	122.9	4.48[c]	13.98	1.36	8.2
2000	9.95	2.92	8.87[c]	13.3	0.076	116.7	8.96[c]	13.23	1.61	7.8
2100	9.3	3.23	8.14[c]	13.3	0.08	124.1	3.43[c]	13.13	1.65	8.2
2200	8.55	3.17	2.15		0.076		1.66		1.51	
2300	7.86	2.83	0.99		0.065		1.04		1.33	

[a]Here the sunspot number is R_{12}.
[b]Here EUV12 is in 10^{10} photons cm^{-2} s^{-1}.
[c]Here the significant level is 0.01.

motions. Although the detail causal mechanisms are not fully understood, we find that the F value over Chung-Li, the northern anomaly region, reaches its saturated condition during 1000 and 2100 LT (Table 5). Figures 6 and 7 as well as Table 5 reveal that the F values in $foF2_{12}$ versus R_{12} and $foF2_{12}$ versus EUV_{12} reach the first maxima at ~1200 and 1500 LT and the second maxima at ~1800 and 2000 LT, respectively. *Heelis et al.* [1974] and *Kelley* [1989] found that the ionospheric F region in the anomaly could be significantly affected by the daily fountain effect and prereversal enhancement, and the most pronounced $\mathbf{E} \times \mathbf{B}$ vertical drift around the geomagnetic equator of the two mechanisms are at ~1000–1200 LT and 1700–1900 LT, respectively. *Yeh et al.* [1997] and *Tsai and Liu* [1999] used the electron density depletion that occurred during solar eclipse as a tracer to estimate the time delay of plasma transportation from the magnetic equator to the associated anomaly region. They find that owing to the fountain effect and the prereversal enhancement the time delays are ~3–5 and 1–3 hours, respectively. In this study the time delay between the first and second maxima and the most pronounced $\mathbf{E} \times \mathbf{B}$ vertical drift of the daily fountain effect and the prereversal enhancement are also ~2–5 and 1–3 hours, respectively. The agreement in the time delays between this paper and previous studies indicates that the daily fountain effect and prereversal enhancement in the equatorial region could significantly increase the foF2 and result in the ionosphere been saturated in the equatorial anomaly region.

[17] The ionosphere is very dynamic, and therefore any external forcing results in its response. Figure 8 illustrates that two maxima in the standard deviation and the two slopes curves concurrently occurred at 1100 and 2100 LT. It might be also reasonable to assume that two maxima are related to the fountain effect and prereversal enhancement related since the upward $\mathbf{E} \times \mathbf{B}$ drifts of the two mechanisms in the equatorial and off-equator regions could significantly perturb the foF2 of the equatorial anomaly region.

[18] Another interesting relationship shown in Figures 6 and 7 is that the change point R_{12} (or EUV_{12}) is inversely proportional to the two quantities of the saturated $foF2_{12}$ and the $foF2_{12}$ mean. This indicates that the ionospheric electron density with a large $foF2_{12}$ mean does not increase with the solar activity ($F10.7_{12}$, R_{12}, or EUV_{12}) but rather has a certain limitation and reaches its saturated condition in an early stage during an strictly rise period of intense solar cycle.

[19] In conclusion, the two-segmented linear model can be employed to quantitatively examine the saturation effects as well as to precisely determine the saturated value and the changing point. It is found that the foF2 saturation effect appears not only for the sunspot but also for EUV radiation. These results confirm that the most profound saturation features in foF2 occur at the equatorial anomaly crest regions. Moreover, the diurnal results suggest that the daily ionospheric equatorial fountain and prereversal enhancement are both important for the saturation features. The goodness of fit of both spatial (latitudinal) distributions and temporal (diurnal, seasonal, and solar activity) variations demonstrate that the denser ionospheric electron density results in the more profound saturation effects.

[20] **Acknowledgments.** This work was partly supported by the National Science Council grant NSC90-2111-M-008-062-AP3 and NSC90-2119-M-008-013 and the Ministry of Education grant 91-N-F07-7-4. The authors wish to thank N. Balan for useful discussions in the first S-RAMP meeting.

[21] Hiroshi Matsumoto and Lou-Chuang Lee thank Tadahiko Ogawa and another reviewer for their assistance in evaluating this paper.

References

Balan, N., G. J. Bailey, and B. Jayachandran, Ionospheric evidence for a nonlinear relationship between the solar e. u. v. and 10.7 cm fluxes during an intense solar cycle, *Planet. Space Sci.*, *41*, 141–145, 1993.

Balan, N., G. J. Bailey, B. Jenkins, P. B. Rao, and R. J. Moffet, Variations of ionospheric ionization and related solar fluxes during an intense solar cycle, *J. Geophys. Res.*, *99*, 2243–2253, 1994a.

Balan, N., G. J. Bailey, and R. J. Moffett, Modeling studies of ionospheric variations during an intense solar cycle, *J. Geophys. Res.*, *99*, 17,467–17,475, 1994b.

Balan, N., G. J. Bailey, and Y. Z. Su, Variations of the ionosphere and related solar fluxes during solar cycles 21 and 22, *Adv. Space Res.*, *18*, (3)11–(3)14, 1996.

Bilitza, D., International Reference Ionosphere 1990, http://www.spenvis.oma.be/spenvis/help/models/iripos/iri90.html, Natl. Space Sci. Data Cent./World Data Cent. A for Rockets and Satellites, Greenbelt, Md., 1990.

Chen, Y. I., J. Y. Liu, and S. C. Chen, Statistical investigation of the saturation effect of sunspot on the ionospheric foF2, *Phys. Chem. Earth*, *25*, 359–362, 2000.

Davies, K., *Ionospheric Radio*, 580 pp., Peter Peregrinus, London, 1990.

Gallant, A. R., and W. A. Fuller, Fitting segmented polynomial regression models whose joint points have to be estimated, *J. Amer. Statist. Assoc.*, *68*, 144–147, 1973.

Gopala Rao, M. S., and R. Samibasiva Rao, The hysteresis in F2-layer parameters, *J. Atmos. Terr. Phys.*, *31*, 1119–1125, 1969.

Hedin, A. E., Correlations between thermospheric density and temperature, solar EUV flux, and 10.7-cm flux variations, *J. Geophys. Res.*, *89*, 9828–9834, 1984.

Heelis, R. A., P. C. Kendall, R. J. Moffett, D. W. Windle, and H. Rishbeth, Electrical coupling of the E-and F-regions and its effect on F-region drifts and winds, *Planet. Space Sci.*, *22*, 743, 1974.

Jones, W. B., and D. L. Obitts, Global representation of annual and solar cycle variation of foF2 monthly median 1954-1958, Off. Telecomm. ITS Res. Rep. 3, U.S. Gov. Print. Off., Washington, D.C., 1970.

Kane, R. P., Sunspots, solar radio noise, solar EUV and ionospheric foF2, *J. Atmos. Terr. Phys.*, *54*, 463–464, 1992.

Kelley, M. C., *The Earth's Ionosphere*, 487 pp., Academic, San Diego, Calif., 1989.

Lakshmi, D. R., B. M. Reddy, and R. S. Dabas, On the possible use of recent EUV data for ionospheric predictions, *J. Atmos. Terr. Phys.*, *50*, 207–213, 1988.

Ratcliffe, J. A., *An Introduction to the Ionosphere and Magnetosphere*, 256 pp., Cambridge Univ. Press, New York, 1974.

Tsai, H. F., and J. Y. Liu, Ionospheric total electron contents response to solar eclipse, *J. Geophys. Res.*, *104*, 12,657–12,668, 1999.

Tobiska, W. K., and C. A. Barth, A solar EUV flux model, *J. Geophys. Res.*, *95*, 8243–8251, 1990.

Yeh, K. C., D. C. Yu, K. H. Lin, C. R. Huang, W. H. Tsai, J. Y. Liu, J. S. Xu, K. Igarashi, C. Xu, and W. X. Wang, Ionospheric response to a solar eclipse in the equatorial anomaly region, *Terr. Atmos. Ocean. Sci.*, *8*, 165–178, 1997.

J. Y. Liu, Institute of Space Science, and Center for Space and Remote Sensing Research, National Central University, Chung-Li 320, Taiwan. (jyliu@jupiter.ss.ncu.edu.tw)

Y. I. Chen and J. S. Lin, Institute of Statistics, National Central University, Chung-Li 320, Taiwan. (ychen@stat.ncu.edu.tw)